

Comparison of ASTER and ETM⁺ data for exploration of porphyry copper mineralization: A case study of Sar Cheshmeh areas, Kerman, Iran

H. Ranjbar¹, H. Shahriari¹, M. Honarmand²,

¹ Department of Mining Engineering, Shahid Bahonar University of Kerman, Iran. Post box No. 76135-133, e-mail: hranjbar64@yahoo.com, Tel and Fax: +98-341-2112764

² Department of Geology, Shahid Bahonar University of Kerman, Iran. Post box No. 76135-133

Abstract

Sar Cheshmeh area is located in the Central Iranian Volcanic Belt. The area is covered mainly by the Eocene volcanic rocks that are intruded by the Oligo-Miocene intrusives. Copper mineralization in the area is mainly of porphyry type and is associated with extensive hydrothermal alteration. ETM⁺ and ASTER data has been analyzed for enhancing the areas with hydrothermal alteration through principal component analysis and Crosta technique. For each data set, iron oxide and hydroxyl images are prepared. The comparison of these images for ASTER and ETM⁺ data on this study area showed that ASTER data has better capability for recognition of hydrothermal alteration and lithological discrimination.

Key words: ASTER, ETM⁺, alteration, Crosta method, porphyry mineralization, Iran

Introduction

The study area is located in the southern part of Central Iranian Volcanic Belt. This belt has a great potential as far as porphyry copper mineralization is concerned. Darrehzar and Sar Cheshmeh porphyry copper deposits are presently mined for Cu, and Mo in the area. The area has a semi-arid type of climate and has a mountainous topography. Vegetation cover is substantially poor in the area.

Porphyry type deposits are associated with hydrothermal alterations such as phyllic, argillic, potassic and propylitic. Hydroxyl minerals are abundant in the phyllic, argillic and potassic zones. At the same time, an oxide zone is developing over many of the porphyry bodies, which are rich in iron oxide minerals. These alteration minerals can be detected by remote sensing techniques. Hydroxyl and iron oxide minerals can be identified through remote sensing techniques (e.g. Rutz-Armenta and Prol-Ledesma, 1998; Tangestani and Moore, 2001).

Landsat data has been used for a number of years in arid and semi-arid environments to locate areas of iron oxides and/or hydrous minerals which might be associated with hydrothermal alteration zones. ASTER sensor onboard Terra platform has more capability in terms of spatial and spectral resolution than Landsat. Theoretically, the SWIR bands of ASTER have more capability than the landsat for recognition of areas with hydrothermal alteration (Figure 1). This study aims at evaluating ASTER and ETM⁺ data for enhancing the areas with hydrothermal alteration.

Different workers have used ASTER data for geological mapping in recent years (Danishwar, 2001; Abdeen et al., 2001; Rowan and Mars, 2001; Abrams, 2002; Liu and Mason, 2002; Yoshiki, N., 2002).

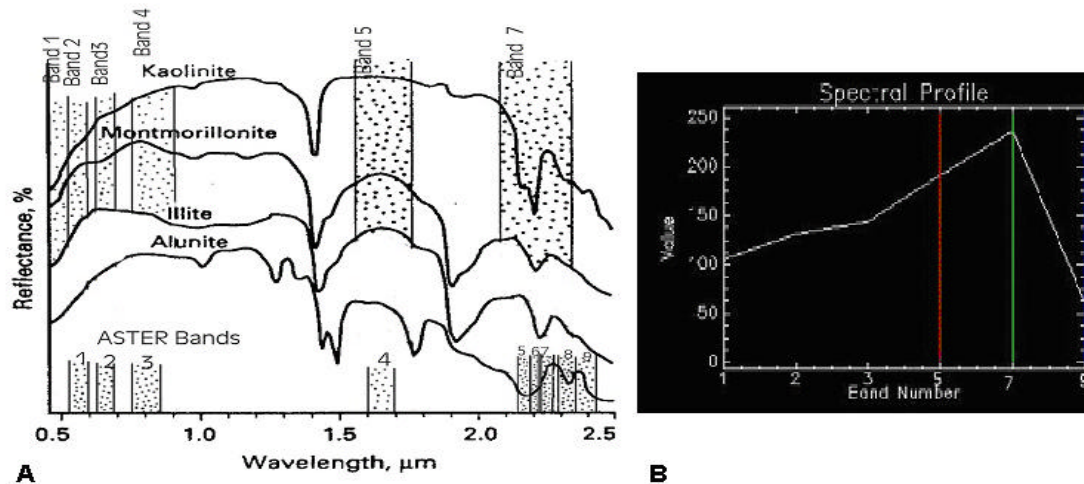


Figure 1: A) Spectra of hydroxyl bearing minerals(after Hunt, 1979). Bandwidths of TM and ASTER are shown. B) Relative reflectance for ASTER bands over an altered area .

Geology of the area

The volcanic-sedimentary rocks of Eocene age are the oldest rocks in the Sar Cheshmeh area represented by pyroclastics, pyroxene trachyandesites, pyroxene andesites, trachyandesites, trachybasalts and andesites. The sedimentary rocks in the volcanic-sedimentary complex are mainly sandstone and less frequently limestone that has subordinate development in the area. The Eocene volcanic sedimentary rocks are intruded by Oligocene-Miocene plutonic rocks that consist of mainly granodiorite, quartz-diorite, diorite, monzonite, tonalite and granite. The volcanic rock in the immediate vicinity of these intrusives are widely metamorphosed and altered. Most of the plutonic and volcanic rocks are hydrothermally altered and at places they are mineralized. Argillization, sericitization and propylitization are the most common types of hydrothermal alteration in the area. The Neogene sediments consist of mainly loosely consolidated, unsorted and poorly stratified conglomerate and sandstone overlying the Eocene volcanic-sedimentary rocks. Calcareous terraces, dacitic rocks and recent alluvium are the main Quaternary features in the area.

Data analysis

The principal component transformation is a multivariate statistical technique that selects uncorrelated linear combinations (eigenvector loadings) of variables in such a way that each successively extracted linear combination, or principal component(PC), has a smaller variance. The principal component analysis is widely used for alteration mapping in metallogenic provinces. Crosta technique is also known as feature oriented principal components selection. Through the analysis of the eigenvector values it allows identification of the principal components that contain spectra information about specific minerals, as well as the contribution of each of the original bands to the components in relation with spectral response of the materials of interest. This technique indicates whether the materials are represented bright or dark pixels in the principal components according with the magnitude and sign of the eigenvectors loadings. This technique can be applied on ETM+ and ASTER data.

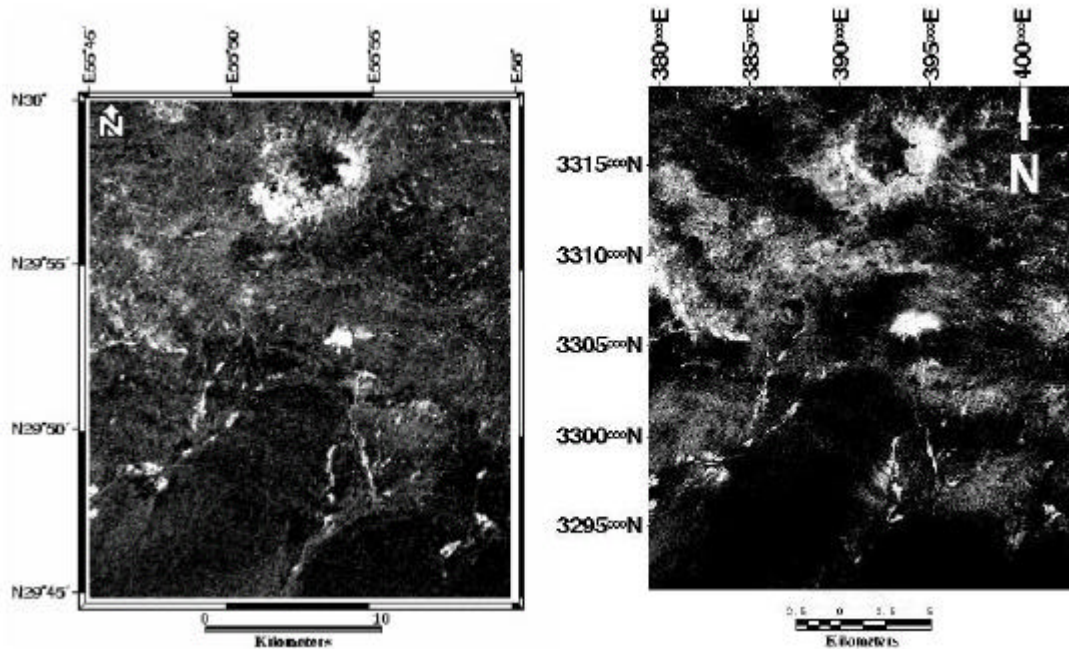


Figure 2: Left image shows the Landsat image prepared by using the eigenvector loadings of PC4. Right image shows the ASTER image prepared by using eigenvector loadings of PC2. In both images bright pixels are the altered areas.

Table 1: Eigenvector loadings, eigenvalues and percentage of variance of the principal components for six bands of ETM

	PC1	PC2	PC3	PC4	PC5	PC6
Band1	0.2	-0.5	-0.3	-0.4	-0.4	-0.6
Band2	0.3	-0.4	-0.2	-0.3	0.1	0.8
Band3	0.4	-0.4	0.2	0.3	0.6	-0.2
Band4	0.4	0.0	0.8	-0.1	-0.4	0.0
Band5	0.6	0.5	-0.1	0.5	0.4	-0.2
Band7	0.5	0.3	-0.4	-0.5	-0.5	0.2
Variance %	91.2	6.2	1.6	0.46	0.36	0.12

Principal component analysis is done using six ETM+ bands as input Bands (Table 1). The first principal component does not contain spectral features relevant in this analysis, as it is a combination of all Bands. This component contains 91.2 per cent of the variance of six bands. This PC gives information mainly on albedo and topography. Vegetation is enhanced in PC3 as this PC has higher loading of Band-4 (0.84). PC4 enhances the hydroxyl minerals. This PC has higher loadings of Bands 5 (0.51) and 7 (-0.51) but with opposite signs. Hydroxyl image that is prepared by using eigenvector loadings of PC4 is shown in Figure 2. A similar analysis of PC5 shows that the most important contributions come from TM1(-0.43) and TM3(0.64). According to spectral characteristics of iron oxide, it follows that iron oxide will be mapped by bright pixels. Iron oxide image is obtained by using eigenvector loadings of PC5.

Similar analysis is done on ASTER data. The first PC shows the albedo. PC2 enhances the hydroxyl bearing areas as this PC has higher loadings of bands 5 and 7 with plus sign and band 9 with negative sign. As band 9 shows absorption over altered areas, this PC can enhance the altered areas.

Table 2 : Eigenvector loadings of principal components for ASTER data

	PC1	PC2	PC3	PC4	PC5	PC6
Band1	0.2	-0.1	-0.8	-0.1	-0.4	-0.4
Band2	0.6	-0.2	0.2	0.4	0.4	-0.5
Band3	0.4	0.4	0.4	-0.5	-0.4	-0.3
Band5	0.3	0.3	-0.3	-0.4	0.7	0.3
Band7	0.5	0.4	-0.1	0.5	-0.3	0.5
Band9	0.4	-0.8	0.1	-0.3	-0.2	0.4

ETM⁺ and ASTER data has been analyzed for enhancing the areas with hydrothermal alteration through principal component analysis and Crosta technique. For each data sets hydroxyl image is prepared (Figure 2). The comparison of these images for ASTER and ETM⁺ data on this study area showed that ASTER data has better capability for recognition of hydrothermal alteration.

Conclusions

Comparison of Landsat and ASTER data over known altered areas shows that ASTER data has more capability than Landsat data for enhancing areas with hydrothermal alteration.

Acknowledgement

ASTER data has been provided by Earth Remote Sensing Data Analysis Center, Japan. The Kerman office of Mines and Industries has supported this project.

References:

- Abdeen, M. M. , Thurmond, A. K., Abdelsalam, M. G., 2001. Application of ASTER band ratio images for geological mapping in arid regions: the Neoproterozoic Allaqi Suture, Egypt, GSA Annual Meeting, November 2001, USA.
- Abrams, M., 2002. ASTER user handbook. Jet Propulsion Lab.
- Amos, B., J., Greenbaum, D., 1989. Alteration detection using TM imagery, the effects of supergene weathering in an arid climate, *International Journal of Remote Sensing*, 10: 515-527.
- Danishwar, S., 2001. Interpretation of ASTER remote sensing data on northwest Kohistan Terrain, Pakistan Himalayas, GSA Annual Meeting, November 2001, USA.
- Geological Society of Iran, 1973. Exploration for ore deposit in Kerman Region. GSI report YU/53, 220 p.
- Hunt, G. R., 1979. Near-Infrared spectra of alteration minerals potential for use in remote sensing. *Geophysics*, 44: 1974-1986.
- Liu, Y. G. and Mason, P. J., 2002. Hydrothermal alteration mapping in epithermal gold deposits of Abanicos Trend, Argentina, using ASTER data, [www. Ese.ic.ac.uk](http://www.Ese.ic.ac.uk).
- Rowan, L. C., and Mars, J. C., 2001. Initial lithologic mapping results using Advanced Space borne Thermal Emission and Reflection Radiometer (ASTER) data, EOS, Transactions American Geophysical Union, Spring Supplement, Abstract U31A-05.
- Rutz-Armenta, J. R. and Prol-Ledesma, R. M., 1998. Techniques for enhancing the spectral response of hydrothermal alteration minerals in Thematic Mapper images of Central Mexico, *International Journal of Remote Sensing*, 19: 1981-2000.
- Tangestani, m. H. and Moore, F., 2001. Comparison of three principal component analysis techniques to porphyry copper alteration mapping: A case study, Meiduk area, Kerman, Iran, *Canadian Journal of remote Sensing*, 27: 176-181.
- Yoshiki, N., 2002. Rock type mapping with indices defined for multispectral thermal infrared ASTER data: Case studies, Proceedings of Remote Sensing for Environmental Monitoring, GIS Applications, and Geology II, Sep 23-26 2002, Agia Pelagia, Greece, SPIE. v 4886, 2002, p 123-132.